The effect of attractive monomer-monomer interactions on adsorption of a polymer chain

1991 J. Phys. A: Math. Gen. 24 827

(http://iopscience.iop.org/0305-4470/24/4/016)

J. Phys. A: Math. Gen. 24 (1991) 827–849. Printed in the UK

The effect of attractive monomer–monomer interactions on the adsorption of a polymer chain

A R Veal†, J M Yeomans† and G Jug‡§

† Department of Theoretical Physics, Oxford University, Oxford OX1 3NP, UK
‡ Theory and Computational Science Group, AFRC-IFRN, Colney Lane, Norwich NR4 7UA, UK
§ International School for Advanced Studies (SISSA), Strada Costiera 11, 34014 Trieste, Italy

Received 23 July 1990, in final form 10 October 1990

Abstract. We have used transfer matrix techniques to study a model of polymer adsorption and collapse. We consider the conventional model of a self-avoiding walk with attractive nearest-neighbour interactions on the square lattice and introduce adsorbing boundaries. The numerical results are consistent with the existence of a multicritical point where the adsorption and collapse transitions coincide and suggest that the adsorption transition of a collapsed polymer chain is *first order*. There is also clear evidence that the collapse transition lowers the adsorption temperature. Estimates of the surface scaling dimensions at the ordinary-Θ transition support the conjecture of Seno and Stella that the *surface* critical behaviour at the Θ and Θ' points belong to different universality classes.

1. Introduction

The mathematical modelling of polymer conformations in the presence of adsorbing substrates is a topic of great practical interest in the applied sciences (see, e.g., [1]). The problem acquires added importance when the polymer molecule presents the possibility of a collapse (coil–globule, protein folding) transition when dissolved in a bulk solvent; the situation with an adsorbing substrate then becomes relevant to both colloidal stabilization by biopolymers [2] and membrane biophysics [3]. At the same time, these problems (taken separately) have attracted a good deal of attention in statistical mechanics [4–6].

With the advent of conformal-invariance techniques [7], the critical exponent structure of two-dimensional polymer models has become an area of active research. Recent reviews by Duplantier (for example, [8]) contain *exact* expressions for the exponents describing the surface adsorption and bulk collapse of polymers in two dimensions. However, there is a less complete understanding of models with competing monomer–surface and monomer–monomer interactions where the collapse and adsorption transitions may occur simultaneously. The new class of models are interesting not only for the possible changes in the universality class(es) but also for the structure of the ensuing phase diagram.

Bouchaud and Vannimenus [9] have looked at an exactly solvable interacting random walk model of a polymer embedded in a three-dimensional fractal lattice and

0305-4470/91/040827+23$03.50

adsorbing at an attractive lattice surface. Beside the expected adsorption transition, a collapse transition is seen to occur for the adsorbed random walk. The present authors [10] have also presented an account of a large-size transfer matrix study of the phase diagram of a *directed* interacting random walk on a square lattice adsorbing to an edge. In both of these studies, the phase diagram includes the interesting feature of a *first-order* adsorption phase transition for the collapsed chain, at least within a range of parameter values.

In this paper, we present a transfer matrix study of an *isotropic* self-avoiding walk model with nearest-neighbour interactions on a square lattice. We extend Saleur's earlier treatment of the collapse transition in the bulk [11] by introducing attractive interactions at the edges of the strip. Following a careful analysis of the adsorption transition in the absence of nearest-neighbour interactions (which complements the recent work of Guim and Burkhardt [12]), we report the results of a study of the model when both adsorption and collapse transitions may occur. Our results are consistent with the existence of a multicritical point where adsorption and collapse coexist, thus corroborating the small-cell renormalization results of a parallel study for a related geometrical model of polymer collapse near interfaces [13]. We believe that the concomitance of these results suggests a richness of behaviour in a realistic model of protein folding at interfaces and hope that our efforts may stimulate further more precise studies, perhaps using Monte Carlo or conformal invariance techniques. We also calculated the surface exponents for the ordinary collapse transition. Our results appear to support the controversial results of a recent Monte Carlo study by Seno and Stella [14].

The remainder of the article is organized as follows. In the next section we introduce the model and define the transfer matrix. Section 3 reviews the adsorption transition for a polymer chain without monomer–monomer interactions. Exponent values are calculated and compared with those obtained by Guim and Burkhardt [12] by a similar technique. The phase diagram and order parameter for the transition are also discussed. Having established our approach, section 4 contains a study of the model with nearest-neighbour attractive interactions between monomers included. Results for the collapse and adsorption transitions are presented, giving evidence for the existence of a multicritical point in the parameter space where the adsorption and collapse transitions coincide. In section 5 we report results for the surface exponents at the ordinary collapse transition. Finally, section 6 contains our conclusions.

2. The transfer matrix

We consider self-avoiding walks (SAW) on a strip of width L with fixed boundary conditions, as shown in figure 1(a). Monomer–monomer interactions are introduced in the standard way by assigning an energy, $-\varepsilon_B$, to each pair of nearest-neighbour sites visited by the walks (excluding consecutive sites in the same walk) and the attraction of the surface is modelled by an energy, $-\varepsilon_S$, for each step along either edge of the strip. The generating function of the model can be written as

$$\mathcal{Z}_L = \sum_{\text{walks}} K^N Q^{N_S} P^{N_B} \tag{1}$$

where K is the monomer fugacity, $Q = \exp(\varepsilon_S/k_BT)$, $P = \exp(\varepsilon_B/k_BT)$, N counts the total number of steps in the walks, N_S the number of steps at the surface and N_B the number of nearest-neighbour interactions (see figure 1(a)).

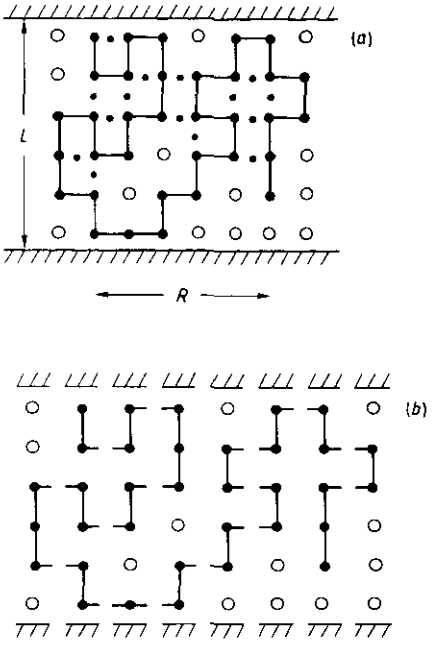

Figure 1. (*a*) A self-avoiding walk on a strip of width $L = 6$. Monomer–monomer interactions are represented by dots between lattice sites visited by the walk, [• · •]. The walk shown has $N = 33$ steps, with $N_S = 4$ at the surface and there are $N_B = 15$ nearest-neighbour interactions. The end-to-end distance measured along the strip, R, equals 5. (*b*) The self-avoiding walk decomposed into a sequence of columns.

To calculate $\mathcal{Z}_L$ we write equation (1) in terms of a transfer matrix, $\mathbf{T}$, [15]. The first step is to divide all SAW configurations on a strip into a sequence of columns: figure 1(*b*) shows the decomposition of the walk in figure 1(*a*). The set of allowed column states then forms a basis for the transfer matrix. Transfer matrix elements, $\mathbf{T}_{jk}$, are labelled by the states of consecutive columns, j and k, and are defined as

$$\mathbf{T}_{jk} = K^{N_{jk}} Q^{N_{jk}^S} P^{N_{jk}^B} \tag{2}$$

if j and k may be connected to form a section of a SAW, or else

$$\mathbf{T}_{jk} = 0. \tag{3}$$

N_{jk}, N_{jk}^S and N_{jk}^B are the numbers of steps, surface steps and interactions, respectively, between the centres of columns j and k.

The partition function for walks with ends in the zeroth and Rth columns can be written in terms of the transfer matrix as

$$\mathcal{Z}_{L,R} = \boldsymbol{v}^{\mathrm{t}} \mathbf{T}^R \boldsymbol{u} \tag{4}$$

where $\boldsymbol{u}$ and $\boldsymbol{v}$ are vectors which depend on the initial and final positions of the walks and R is the end-to-end distance measured *along* the strip (figure 1(*a*)). Summing over all R gives the generating function

$$\mathcal{Z}_L = \sum_R \mathcal{Z}_{L,R}. \tag{5}$$

As $R \to \infty$, the expression for $\mathcal{Z}_{L,R}$ (equation (4)) is dominated by the largest eigenvalue of the transfer matrix, λ_L, and the partition function is given by [15]

$$\mathcal{Z}_{L,R} \sim (\lambda_L)^R \qquad \text{as} \quad R \to \infty. \tag{6}$$

Hence, the generating function $\mathcal{Z}_L$ diverges as $\lambda_L \to 1^-$. The singularity in $\mathcal{Z}_L$ is due to the divergence of the average length of the SAW, $\langle N \rangle_L$, and defines the critical fugacity, $K_{c,L}$, for a strip of width L [11]:

$$\lambda_L \left[K_{c,L}(P,Q) \right] = 1. \tag{7}$$

'Thermodynamic' properties of very long polymers on strips follow from the partition function $\mathcal{Z}_{L,R}$ in the limits $R \to \infty$ and $\langle N \rangle_L \to \infty$. From the relations above, one deduces the following expressions for thermodynamic quantities, where the derivatives are evaluated at the points where $\lambda_L = 1$:

$$\frac{\langle N \rangle_L}{R} = \frac{\partial \ln \lambda_L}{\partial \ln K} \tag{8}$$

$$\frac{\langle N_S \rangle_L}{R} = \frac{\partial \ln \lambda_L}{\partial \ln Q} \tag{9}$$

$$\frac{\langle N_B \rangle_L}{R} = \frac{\partial \ln \lambda_L}{\partial \ln P}. \tag{10}$$

An approximation to the true thermodynamic limit, $L \to \infty$, is reached by extrapolating finite-size data.

We have considered the cases of one or two SAW on the strip. The largest eigenvalues, λ_L^i, of the resulting transfer matrices, $\mathbf{T}_L^i$, determine characteristic lengths along the strip

$$\xi_L^{\parallel,i} = -\left(\ln \lambda_L^i\right)^{-1} \tag{11}$$

where i is the number of SAW. Because the problem of SAW on a lattice is equivalent to the O(n) model in the limit $n \to 0$ [16], the lengths $\xi_L^{\parallel,i}$ can be identified with the spin–spin ($i = 1$) and energy–energy ($i = 2$) correlation lengths of a magnetic model. As $K \to K_{c,L}$, both the correlation lengths and the average length of the SAW diverge.

At a critical point of the O(n) model on a semi-infinite lattice, the correlation lengths of both bulk and surface quantities diverge and the statistical properties of the system are conformally invariant. In two dimensions, the semi-infinite system at criticality may be transformed to an infinitely long strip by a conformal mapping. Spin–spin ($i = 1$) and energy–energy ($i = 2$) correlations decay exponentially in the new geometry with

$$\lim_{L \to \infty} \left(\xi_L^{\parallel,i} \right) = \frac{L}{\pi x_S^i} \tag{12}$$

where x_S^i are the surface scaling dimensions of the spin ($i = 1$) and energy ($i = 2$) operators [17]. Hence, the surface scaling dimensions of the O(n) model in the limit $n \to 0$ may be calculated from the transfer matrices for SAW [18].

3. The adsorption transition

We begin by considering polymer adsorption in the good solvent regime, where monomer–monomer interactions may be neglected. At a characteristic temperature, T_A, the average number of monomers adsorbed at the surface, $\langle N_S \rangle$, becomes macroscopic

$$\langle N_S \rangle \sim \langle N \rangle^{\phi_S} \qquad \text{as} \quad \langle N \rangle \to \infty \tag{13}$$

which defines the surface crossover exponent, ϕ_S. Below T_A, a finite fraction of monomers in a polymer chain are adsorbed and polymers are bound to the surface. Above T_A, $\langle N_S \rangle$ remains finite as $\langle N \rangle \to \infty$.

The critical properties of the polymer phases are described by three fixed-points, which all have analogues in the O(n) model in the limit $n \to 0$ [19,20]: (i) the ordinary fixed-point, $(K_c, Q_c^{\mathrm{Ord}})$, governs the behaviour of the unbound phase, where surface interactions are *irrelevant* (in the RG sense); (ii) the special fixed-point, (K_c, Q_c^{Sp}), describes the adsorption transition, with $Q_c^{\mathrm{Sp}} = \exp(\varepsilon_S / k_B T_A)$; and (iii) the surface fixed-point, $(Q \to \infty)$, governs the bound phase.

The critical fugacity at the ordinary and special fixed-points, K_c, is equal to the d-dimensional bulk value. In the bound phase, $Q > Q_c^{\mathrm{Sp}}$, the critical fugacity is a function of Q; near the adsorption transition [20]

$$K_c(Q) - K_c \sim \left| Q - Q_c^{\mathrm{Sp}} \right|^{1/\phi_S} \qquad \text{as} \quad Q - Q_c^{\mathrm{Sp}} \to 0^+ \tag{14}$$

while for large Q

$$K_c(Q) \sim Q^{-1} \qquad \text{as} \quad Q \to \infty. \tag{15}$$

The crossover in the polymer's critical behaviour at the adsorption transition can be associated with the divergence of the average distance a polymer extends from the surface into the bulk, $\xi^{\perp}$. In the bound phase, $\xi^{\perp}$ defines the average thickness of the adsorbed layer at the surface. At the adsorption transition, $\xi^{\perp}$ diverges

$$\xi^{\perp} \sim \left| Q - Q_c^{\mathrm{Sp}} \right|^{-\nu_S} \qquad \text{as} \quad Q - Q_c^{\mathrm{Sp}} \to 0^+ \tag{16}$$

which defines the surface exponent ν_S. In the unbound phase, $Q < Q_c^{\mathrm{Sp}}$, $\xi^{\perp}$ diverges like the bulk correlation length

$$\xi^{\perp} \sim |K - K_c|^{-\nu} \qquad \text{as} \quad K - K_c \to 0^- \tag{17}$$

where ν is the standard bulk exponent. The surface crossover exponent, ϕ_S, is given by the ratio of the bulk and surface exponents [20]

$$\phi_S = \nu / \nu_S. \tag{18}$$

For a strip of width L, the lengths $\xi_L^{\parallel,i}$ defined in the last section obey the finite-size scaling form [21]

$$L^{-1} \xi_L^{\parallel,i}(K,Q) = F^i \left[L^{y}(K - K_c), L^{y_S}(Q - Q_c) \right] \tag{19}$$

as $(K,Q) \to (K_c,Q_c)$ at the ordinary and special fixed-points. F^i are scaling functions and the exponents $y = \nu^{-1}$ and $y_S = \nu_S^{-1}$. From conformal invariance (relation (12)) we have

$$F^i(0,0) = \left(\pi x_S^i\right)^{-1}. \tag{20}$$

The scaling dimensions, x_S^i, are related to standard surface critical exponents by scaling relations [20]:

$$\eta_{\|} = 2x_S^1 \qquad 2\gamma_1 = \gamma + \nu\left(2 - \eta_{\|}\right) \qquad \gamma_{11} = \nu\left(1 - \eta_{\|}\right) \tag{21}$$

and

$$y_S = 1 - x_S^2 \qquad \phi_S = \nu y_S. \tag{22}$$

The exact values of all the exponents at the ordinary and special fixed-points in two dimensions have been determined by Duplantier and Saleur from Coulomb gas mappings and conformal-invariance results (and references therein [8]). The same exponents have also been obtained by Burkhardt, Eisenriegler and Guim from a calculation of the energy–energy correlation function of the semi-infinite O(n) model [22]. Also, K_c is known to high accuracy for the square lattice from the series expansions of Guttmann and Enting [23]:

$$K_c = 0.379\,052\,28 \pm 0.000\,000\,14. \tag{23}$$

Hence, this section should primarily be considered as an introduction to the methods we shall use to study the SAW model when monomer–monomer interactions are included. The absence of nearest-neighbour interactions ($\varepsilon_B = 0$ in this section) allows us to use a simpler set of configurations as a basis for the transfer matrix [15] and hence results for larger strip widths can be presented.

We have used phenomenological renormalization group methods [21,24] to determine the ordinary and special fixed-points. Recurrence relations for the coupling constants are defined by relating correlation lengths on strips of successive widths. Estimates of the critical couplings are then obtained from the fixed-points, K^* and Q^*. The results improve as larger strip widths are used.

Finite-size estimates of the critical line above the adsorption transiton, $K_L^*(Q)$, follow from the solutions of the two-strip renormalization equations

$$L^{-1}\xi_L^{\|,1}\left[K_L^*(Q)\right] = (L-1)^{-1}\,\xi_{L-1}^{\|,1}\left[K_L^*(Q)\right]. \tag{24}$$

Figure 2(a) shows $K_L^*(Q)$ and figure 2(b) shows the correlation length amplitude along the critical line, $A_L^1(Q)$, defined by

$$A_L^1(Q) = \frac{2L}{\pi\xi_L^{\|,1}\left[K_L^*(Q)\right]}. \tag{25}$$

One can clearly identify the ordinary and special fixed-points from the crossing points of the curves.

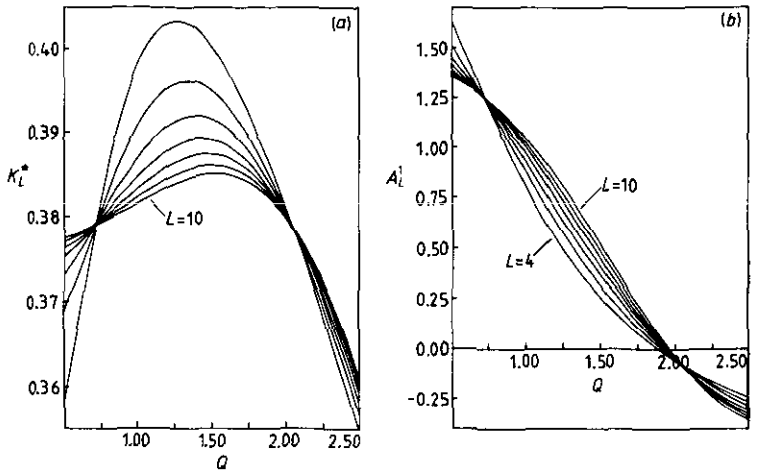

Figure 2. Finite-size estimates of (*a*) the critical line, $K_L^\star(Q)$, and (*b*) the correlation length amplitude along the critical line, $A_L^1(Q)$, obtained by two-strip renormalization. The location of the ordinary and special fixed-points can be identified from the crossing points of either graph.

Table 1. Fixed-point couplings and critical exponents obtained from the one-SAW transfer matrix using equations (26) and (27).

	L	$K_L^\star$	$Q_L^\star$	y^L	y_S^L	$\eta_\parallel^L$
Ordinary	5	0.379 3930	0.721 2606	1.3337	−1.0998	1.237 315
fixed-point	6	0.379 1943	0.717 1025	1.3339	−1.0558	1.242 670
	7	0.379 1222	0.714 6268	1.3339	−1.0359	1.245 223
	8	0.379 0913	0.713 0392	1.3338	−1.0252	1.246 592
	9	0.379 0764	0.711 9533	1.3337	−1.0186	1.247 397
	10	0.379 0683	0.711 1675	1.3336	−1.0144	1.247 909
Special	5	0.378 0639	2.063 116	1.3194	0.663 20	−0.090 510 91
fixed-point	6	0.378 7182	2.047 802	1.3285	0.680 88	−0.082 521 07
	7	0.378 9424	2.041 773	1.3330	0.688 40	−0.078 871 68
	8	0.379 0299	2.039 134	1.3354	0.691 70	−0.077 071 04
	9	0.379 0667	2.037 908	1.3367	0.693 04	−0.076 145 60
	10	0.379 0824	2.037 339	1.3376	0.693 40	−0.075 676 94

Finite-size estimates for the critical couplings at the ordinary and special transitions are given by the fixed-points, $(K_L^\star, Q_L^\star)$, of the three-strip renormalization equations

$$L^{-1}\xi_L^{\parallel,1}(K_L^\star, Q_L^\star) = (L-1)^{-1}\,\xi_{L-1}^{\parallel,1}(K_L^\star, Q_L^\star) = (L-2)^{-1}\,\xi_{L-2}^{\parallel,1}(K_L^\star, Q_L^\star)\,. \tag{26}$$

The exponents y and y_S are obtained by linearizing around the fixed-point [25]. In addition, we have

$$\eta_\parallel^L = \frac{2L}{\pi\xi_L^{\parallel,1}(K_L^\star, Q_L^\star)}\,. \tag{27}$$

Results for the fixed-points and critical exponents are shown in table 1.

The finite-size data in table 1 were extrapolated by assuming an *effective* power law convergence [26]

$$K_L^\star - K_c \sim L^{-v} \qquad \text{as} \quad L \to \infty. \tag{28}$$

The exponent v is calculated from three consecutive finite-size estimates; each triplet $(K_{L-1}^\star, K_L^\star, K_{L+1}^\star)$ then determines a new value $\tilde{K}_L^\star$ in the $L \to \infty$ limit [27]. Results for $\tilde{K}_L^\star$, $\tilde{Q}_L^\star$, $\tilde{y}_S^L$ and $\tilde{\eta}_\parallel^L$ are shown in table 2. The new sequence of estimates are weakly dependent on L and our final estimates of the $L \to \infty$ limits were obtained by plotting the original and extrapolated sequences against $L^{-\tilde{v}}$, where $\tilde{v}$ was an integer value which gave a smooth convergence. The $L \to \infty$ limits, with our estimated error bars for the last digit shown, are given in table 2 together with the exact values of the surface exponents. The error quoted is an estimate of the uncertainty in the *extrapolation* of the finite-size sequences and does *not* take account of the *systematic* errors in the original sequences.

Table 2. Extrapolated values obtained from the finite-size estimates in table 1, as described in the text. The new sequence of estimates are weakly dependent on L. The table gives our final estimates of the $L \to \infty$ limit.

	L	$\tilde{K}_L^\star$	$\tilde{Q}_L^\star$	$\tilde{y}_S^L$	$\tilde{\eta}_\parallel^L$
Ordinary	6	0.3790596	0.70806	−1.0099	1.24896
fixed-point	7	0.3790574	0.70809	−1.0053	1.24905
	8	0.3790567	0.70791	−1.0033	1.24915
	9	0.3790547	0.70761	−1.0023	1.24926
	∞	0.379052 ±0.000002	0.7075 ±0.0005	−1.000 ±0.001	1.2495 ±0.0005
	Exact			−1	5/4
Special	6	0.379120	2.0357	0.6971	−0.07400
fixed-point	7	0.379111	2.0361	0.6955	−0.07442
	8	0.379104	2.0364	0.6943	−0.07473
	9	0.379098	2.0367	0.6936	−0.07501
	∞	0.37908 ±0.00002	2.037 ±0.001	0.694 ±0.001	−0.0755 ±0.0005
	Exact			2/3	−1/12

For the ordinary fixed-point, the sequences of finite-size estimates in table 1 converge in a regular way towards the expected values and even small strips give rather accurate numerical results. The extrapolated values in table 2 are in excellent agreement with exact results and the estimate of K_c compares well with the series result (23).

For the special fixed-point, where there are two relevant parameters, the situation is less clear. The finite-size sequences in table 1 converge monotonically, but the exact values of the exponents lie *between* the numerical results for $L = 5$ and $L = 10$; hence, our extrapolations must contain systematic errors in this case. For larger strips ($L \gg 10$) we would expect the finite-size sequences to converge towards the values for the semi-infinite system. However, the finite-size estimates show an accuracy

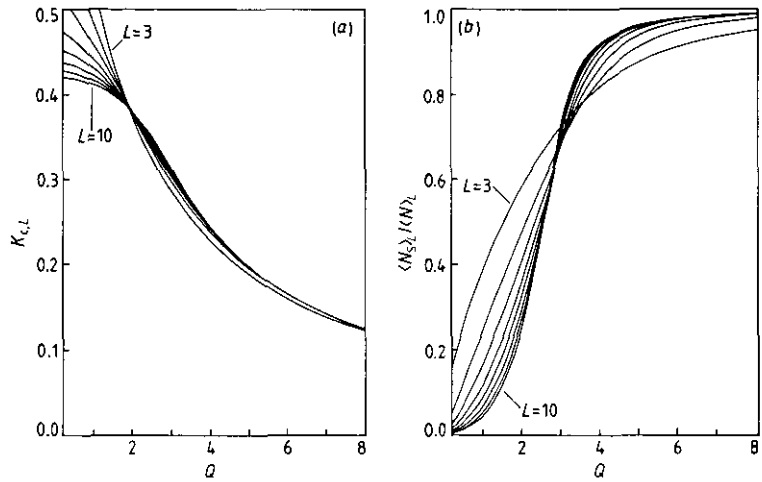

Figure 3. Finite-size estimates of (*a*) the critical line, $K_{c,L}(Q)$, and (*b*) the fraction of adsorbed monomers at criticality, $\langle N_S \rangle_L / \langle N \rangle_L$, for one SAW on a strip. The critical lines in (*a*) cross close to the adsorption multicritical point and show a rapid convergence with increasing L within the adsorbed phase.

comparable with other phenomenological renormalization calculations at multicritical points and our estimate of the adsorption threshold, $Q_c^{Sp} = 2.037 \pm 0.001$, is in good agreement with other calculations [12].

Our findings are in excellent agreement with those of Guim and Burkhardt [12], who have presented a related approach to the problem. They studied the fixed-point structure via the two-length, two-strip renormalization relations

$$L^{-1}\xi_L^{\|,1}(K_L^\star, Q_L^\star) = (L-1)^{-1}\,\xi_{L-1}^{\|,1}(K_L^\star, Q_L^\star) \tag{29}$$

$$L^{-1}\xi_L^{\|,2}(K_L^\star, Q_L^\star) = (L-1)^{-1}\,\xi_{L-1}^{\|,2}(K_L^\star, Q_L^\star). \tag{30}$$

This has the advantage of giving both surface scaling dimensions of interest directly from correlation length amplitudes. Guim and Burkhardt also observed irregular convergence of their finite-size data at the special fixed-point. Our three-strip calculations appear to be more accurate at the ordinary fixed-point. We shall employ both two-parameter renormalization methods for the study of the model when nearest-neighbour interactions are included.

A third approach which has proved useful is to study the critical properties of a polymer confined to a strip. From section 2, the finite-size critical fugacity is defined by

$$\lambda_L\,[K_{c,L}(Q)] = 1 \tag{31}$$

while the derivatives of λ_L at $K_{c,L}$ define thermodynamic quantities for long polymers (8), (9). Figure 3(*a*) shows the critical line, $K_{c,L}(Q)$, and figure 3(*b*) shows the fraction of adsorbed monomers at criticality, $\langle N_S \rangle_L / \langle N \rangle_L$, for the case of one SAW. The results are a good approximation for the properties in the bound phase, where the polymer only extends a finite distance into the bulk as $\langle N \rangle \to \infty$. In fact, for $Q \gg Q_c^{Sp}$ the dependence on L is expected to be exponential and the curves very quickly approach their asymptotic values. As the adsorption transition is approached, $Q - Q_c^{Sp} \to 0^+$, finite-size effects appear as the adsorption layer's thickness, $\xi^\perp$, becomes comparable with the strip width, L.

The critical lines, $K_{c,L}(Q)$, cross close to the adsorption multicritical point and the crossing points are expected to converge to (K_c, Q_c^{Sp}) as $L \to \infty$ [10]. Finite-size estimates, $(K_{c,L}, Q_{c,L})$, were obtained from the intersection points for successive strip widths, i.e. from the solutions of the equation

$$\lambda_L^1 (K_{c,L}, Q_{c,L}) = \lambda_{L-1}^1 (K_{c,L}, Q_{c,L}) = 1. \tag{32}$$

The results, together with extrapolated values $(\tilde{K}_{c,L}, \tilde{Q}_{c,L})$, are shown in table 3. Although the numerical results for small strips are not particularly accurate, the sequence of estimates converge regularly to give reliable extrapolated values. Our final estimates, $K_c = 0.3790 \pm 0.0002$ and $Q_c^{Sp} = 2.04 \pm 0.02$, are consistent with the results from phenomenological renormalization.

Table 3. Finite-size estimates of the multicritical adsorption point, $(K_{c,L}, Q_{c,L})$, obtained from equation (32), together with extrapolated values, $(\tilde{K}_{c,L}, \tilde{Q}_{c,L})$. Final estimates of (K_c, Q_c^{Sp}) are also given.

L	$K_{c,L}$	$\tilde{K}_{c,L}$	$Q_{c,L}$	$\tilde{Q}_{c,L}$
4	0.3869673		1.876449	
5	0.3844798	0.38001	1.903069	1.9971
6	0.3831236	0.37963	1.920397	2.0099
7	0.3822775	0.37942	1.932836	2.0186
8	0.3817027	0.37930	1.942330	2.0243
9	0.3812886	0.37923	1.949883	2.0284
10	0.3809773		1.956076	
∞		0.3790 $\pm$0.0002		2.04 $\pm$0.02

The fraction of adsorbed monomers at criticality is an order parameter for the adsorption transition. In the weakly adsorbed phase, $Q \gtrsim Q_c^{Sp}$, we have the important relation [19]

$$\frac{\langle N_S \rangle}{\langle N \rangle} \sim (\xi^{\perp})^{-y(1-\phi_S)} \qquad \text{as} \quad \langle N \rangle \to \infty. \tag{33}$$

On a finite strip

$$\hat{O}_L = \frac{\langle N_S \rangle_L}{\langle N \rangle_L} \sim L^{-\zeta} \qquad \text{as} \quad L \to \infty \quad \text{at} \quad Q_L^A \tag{34}$$

where $\zeta = y(1-\phi_S)$ and Q_L^A is a finite-size estimate of Q_c^{Sp}. Thus, Q_L^A is a solution of the three-strip equation

$$\frac{\ln\left[\hat{O}_L(Q_L^A) \,/\, \hat{O}_{L-1}(Q_L^A)\right]}{\ln[L/(L-1)]} = \frac{\ln\left[\hat{O}_L(Q_L^A) \,/\, \hat{O}_{L-2}(Q_L^A)\right]}{\ln[L/(L-2)]} = -\zeta_L \tag{35}$$

which also defines a finite-size estimate of the exponent ζ, ζ_L. The results, together with the extrapolated values $\tilde{Q}_A^L$ and $\tilde{\zeta}_L$, are shown in table 4. Problems with the data

Table 4. Finite-size estimates of Q_L^A and ζ_L obtained from (35), together with extrapolated values $\tilde{Q}_L^A$ and $\tilde{\zeta}_L$. Final estimates of $Q_A = Q_c^{SP}$ and $\zeta = \gamma(1-\phi_S)$ are shown and the exact value of the exponent is given.

L	Q_L^A	$\tilde{Q}_L^A$	ζ_L	$\tilde{\zeta}_L$
5	1.988 757		0.706 10	
6	2.020 579	2.0505	0.680 20	0.6486
7	2.034 284	2.0484	0.667 65	0.6513
8	2.040 567	2.0472	0.661 28	0.6530
9	2.043 525	2.0464	0.658 01	0.6542
10	2.044 882		0.656 39	
∞		2.046 ±0.001		0.655 ±0.001
Exact				2/3

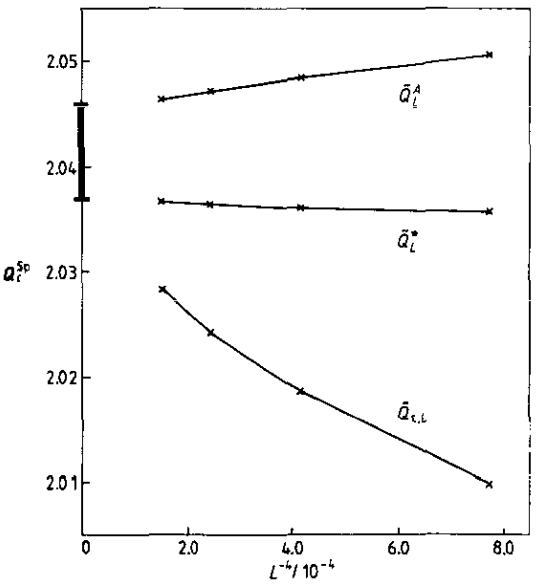

Figure 4. Extrapolated estimates $\tilde{Q}_L^*, \tilde{Q}_{c,L}$ and $\tilde{Q}_L^A$ from tables 2, 3 and 4 plotted against L^{-4}. Extrapolating the curves gives a final estimate $Q_c^{SP} = 2.042 \pm 0.005$.

are the same as those observed with the phenomenological renormalization calculations at the special fixed-point. Our final estimate, $Q_c^{SP} = 2.046 \pm 0.001$, is consistent with our earlier results.

Finally, figure 4 shows the extrapolated estimates $\tilde{Q}_L^*, \tilde{Q}_{c,L}$ and $\tilde{Q}_L^A$ from tables 2, 3 and 4 plotted against L^{-4}. Extrapolating the curves gives upper and lower bounds for the value of Q_c^{SP}. Our final result, $Q_c^{SP} = 2.042 \pm 0.005$, is in excellent agreement with Guim and Burkhardt's final estimate of $Q_c^{SP} = 2.041 \pm 0.002$.

4. Adsorption with collapse

In this section we introduce the effects of solvent-induced monomer–monomer interac-

tions. A polymer now exhibits a collapse transition in the bulk solvent at a characteristic temperature, Θ, [16]. Above Θ, the excluded-volume repulsion between monomers dominates and the polymer has the statistics of a self-avoiding random walk; this is the good solvent regime. Below Θ, attractive interactions dominate and the polymer adopts a compact conformation. Precisely at the Θ point, the polymer has a well defined conformation intermediate between the random and collapsed phases. The universal properties of a polymer at the Θ point are described by the *tricritical* point of the O(n) model in the limit $n \to 0$ [28,29].

In the presence of a substrate with sufficiently attractive monomer–surface interactions, a polymer at the Θ point has an adsorption transition. This occurs at a multicritical point, $(K_c^{\Theta,Sp}, P_c^{\Theta,Sp}, Q_c^{\Theta,Sp})$, in the parameter space where the adsorption and collapse transitions coincide [30].

Figure 5 shows the critical surface, $K = K_c(P,Q)$, projected onto the (P,Q) plane for a two-dimensional polymer. The diagram is *semi-quantitative*: the positions of the phase boundaries can be obtained approximately from the data presented later in this section. The multicritical point, marked M in figure 5, is at the point of intersection of the phase boundaries and separates the adsorption transitions of the ordinary and collapsed SAW phases. As the monomer–monomer interaction parameter P increases, the adsorption transition changes from second to first order at a point T. We expect the points M and T to coincide, as is the case for the exactly solved model of Bouchaud and Vannimenus [9] and also for the directed model [10]. However, one cannot rule out the possibility that T is a tricritical point quite distinct from M occurring on the boundary between the surface SAW and collapsed SAW phases at, say, $P_T \geq 2$, $Q_T \geq 3.5$ (see figure 5). In two dimensions, one expects only one surface SAW phase, because a collapse transition cannot occur in one dimension. Hence, the Θ line separating the ordinary and collapsed phases terminates at the multicritical point M.

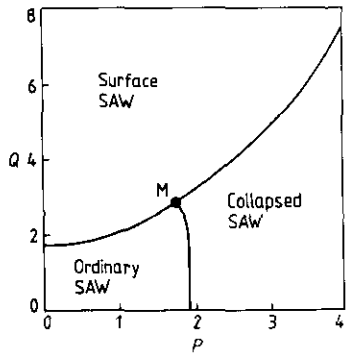

Figure 5. The critical surface, $K = K_c(P,Q)$, projected onto the (P,Q) plane for a two-dimensional polymer. $P = \exp(\varepsilon_B/k_BT)$ and $Q = \exp(\varepsilon_S/k_BT)$ are the Boltzmann factors for the monomer–monomer and monomer–surface interactions, respectively. The multicritical point, M, is at the point of intersection of the phase boundaries and separates the adsorption transitions of the ordinary and collapsed SAW phases. As P increases, the adsorption transition changes from second to first order at a point T. We expect the points M and T to coincide [9,10], but it is possible that T is a tricritical point quite distinct from M occurring on the boundary between the surface SAW and collapsed SAW phases.

The phase boundaries in figure 5 were obtained by studying the critical properties of SAW on strips. There are, however, serious technical difficulties with transfer matrix

calculations at the Θ point. Finite-size data show [11] (i) parity effects—results for odd/even width strips converge in a different way; (ii) poor convergence—estimates converge slowly with increasing size and it is only possible to study narrow strips because of the size of the transfer matrices involved; and (iii) boundary effects—dense polymers are particularly sensitive to boundary conditions [31] and this distorts the finite-size scaling behaviour near the Θ point and in the collapsed phase.

Thus, although we have found convincing evidence for the phase boundaries shown in figure 5, we were not able to obtain very precise estimates from our calculations.

Our best results were obtained by studying the finite-size critical properties of a single SAW. Recall from section 2 that the finite-size critical fugacity is defined by

$$\lambda_L^1 \left[K_{c,L}(P,Q)\right] = 1 \tag{36}$$

with the derivatives of λ_L^1 at $K_{c,L}$ defining the thermodynamic quantities of interest (8)–(10). On a finite strip, the ratio $\langle N_B \rangle_L / \langle N \rangle_L$ will not tend to unity as $P \to \infty$; as the SAW fills all the available sites on the strip

$$\frac{\langle N_B \rangle_L + \langle N \rangle_L}{R(2L-1)} \to 1. \tag{37}$$

We consider first the change in the position of the adsorption transition as a function of the monomer–monomer interaction strength, P. Figures 6 and 7 show the variation in the critical line, $K_{c,L}(Q)$, and the order parameter, $\langle N_S \rangle_L / \langle N \rangle_L$, for strips of width $L = 4$ to 7 for different values of P. For small values of P, the variation of the order parameter with Q suggests that the adsorption transition is second order, whereas for larger P there is strong numerical evidence that the transition is first order. For small P, the position of the transition is well approximated by the crossing points of the curves in figure 6, as was the case for no monomer–monomer interactions (see section 3). However, for larger P, the transition more closely corresponds to the shoulder in the $K_{c,L}(Q)$ curves, where the gradient appears to change discontinuously. Note that, in the adsorbed phase (where one expects an exponential dependence of $K_{c,L} - K_c$ on L) convergence to the $L \to \infty$ limit is very quick. The position of the adsorption phase boundary in figure 5 was estimated, for small P, from the crossing-points (32) and, for large P, from the position of the shoulder in the $K_{c,L}(Q)$ curves. Because only small strip widths can be generated, the estimates are not very precise.

Further evidence for the existence of the multicritical collapse–adsorption point is provided by following the dependence of the collapse transition on the surface interaction parameter, Q. Figures 8 and 9 show the variation in the critical line, $K_{c,L}(P)$, and the collapse order parameter, $\langle N_B \rangle_L / \langle N \rangle_L$, for strips of width $L = 4$ to 7 for different values of Q. For small values of Q, the variation of the order parameter with P is smooth as the tricritical Θ line is crossed. However, for larger Q, there is again strong numerical evidence for a first-order unbinding transition between the surface and collapsed SAW phases. For large Q, the position of the transition is well approximated by the shoulder in the $K_{c,L}(P)$ curves, where the gradient appears to jump discontinously (figure 8). The positions of the shoulder in the $K_{c,L}(P)$ curves give further estimates of the position of the adsorption/unbinding phase boundary in figure 5. In the adsorbed phase, the finite-size results again converge very quickly.

For completeness, we report our attempt to locate the phase boundaries in figure 5 using the analysis of Guim and Burkhardt [12] (discussed in section 3) but with

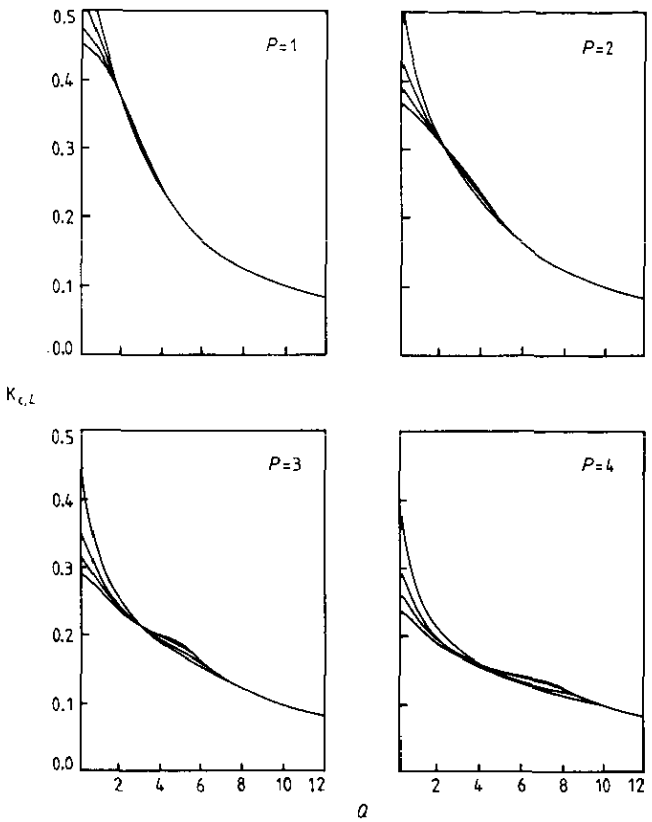

Figure 6. Finite-size estimates of the critical line, $K_{c,L}(Q)$, for strips of width $L =$ 4, 5, 6 and 7 at different values of P.

nearest-neighbour interactions included. Estimates of the coordinates of the adsorption line, $K_L^\star(P)$ and $Q_L^\star(P)$, follow from solutions of the equations

$$L^{-1}\xi_L^{\parallel,1}\left[K_L^\star(P), Q_L^\star(P)\right] = (L-2)^{-1}\,\xi_{L-2}^{\parallel,1}\left[K_L^\star(P), Q_L^\star(P)\right] \tag{38}$$

$$L^{-1}\xi_L^{\parallel,2}\left[K_L^\star(P), Q_L^\star(P)\right] = (L-2)^{-1}\,\xi_{L-2}^{\parallel,2}\left[K_L^\star(P), Q_L^\star(P)\right]. \tag{39}$$

Note that other solutions of the *same* set of equations yield estimates of the coordinates of the Θ line.

Figure 10 shows $Q_L^\star(P)$ for $0.5 < P < 2.5$. The special-SAW fixed-point discussed in section 3 is clearly seen, but, as P increases, finite-size effects become pronounced. For $P \gtrsim 1.6$, the data for strips of odd parity begin to cross over from the adsorption to the Θ line (cf figure 5). However, the crossover behaviour in the vicinity of the multicritical point, (Θ, Sp), is very complicated and our finite-size results are distorted by strong boundary and parity effects. Thus, we cannot give reliable estimates of the location of the multicritical point.

Figures 6–10 provide evidence for the general shape of the phase diagram in figure 5 and also the *approximate* position of the phase boundaries in the parameter space of the model. There is also rather strong numerical evidence that the transition between the surface and collapsed self-avoiding walk phases is *first-order* for large values of P. However, we cannot give the precise location of the multicritical point M or define

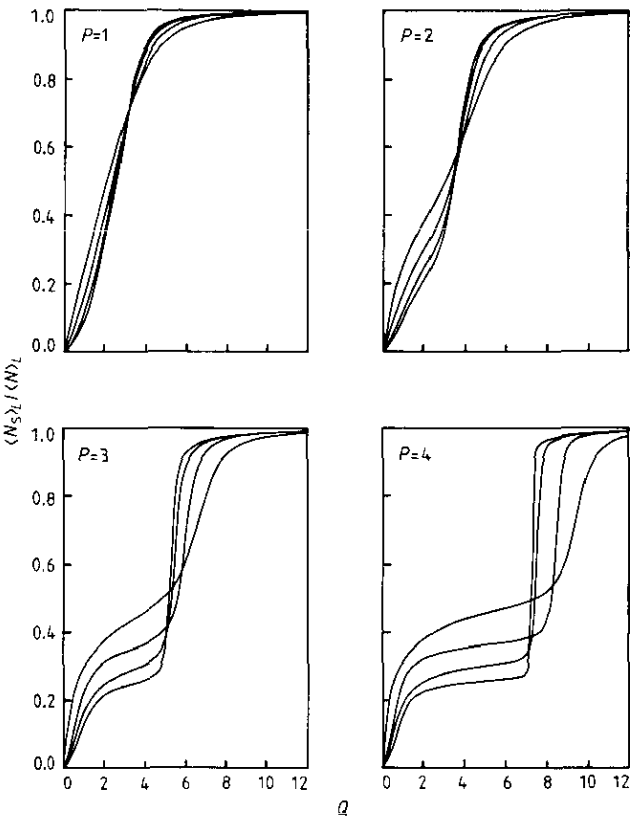

Figure 7. The fraction of adsorbed steps at the critical fugacity, $\langle N_S \rangle_L / \langle N \rangle_L$, for strips of width $L = 4$, 5, 6 and 7 at different values of P. For small values of P, the variation with Q is continuous, while for larger P the results suggest a discontinuous change at the adsorption transition in the thermodynamic limit.

definitively whether it coincides with the point T where the order of the adsorption transition changes.

Physically, a very important question is whether or not the collapse transition is modified by the presence of an adsorbing substrate. At the multicritical collapse–adsorption point, M, the average number of monomers adsorbed at the surface becomes macroscopic and the polymer chain is at the Θ point. In a very small region of the phase diagram near M the collapse transition temperature, Θ, may be shifted due to precursor 'bulk' (meaning relevant to the whole polymer chain) effects induced by the surface potential. This is in marked contrast to the case of the related magnetic system, where the modified surface exchange bonds cannot shift the bulk tricritical temperature. A recent study of a related model of polymer collapse by Cattarinussi and Jug [13] suggests that the Θ temperature is enhanced at the multicritical collapse–adsorption point in both two and three dimensions. This enhancement appears to be much greater than the shift induced by finite-size effects, which thus cannot be easily invoked to explain the results. It has been argued that a shift in Θ is expected because the reduction of the conformational entropy of the random self-avoiding walk phase in the presence of a surface greatly exceeds that of the collapsed phase [32]. If this is the case, we would expect the critical value $P_c = \exp(\varepsilon_B / k_B \Theta)$ to be lower at the multicritical point, M, than at the bulk collapse transition. However, our results

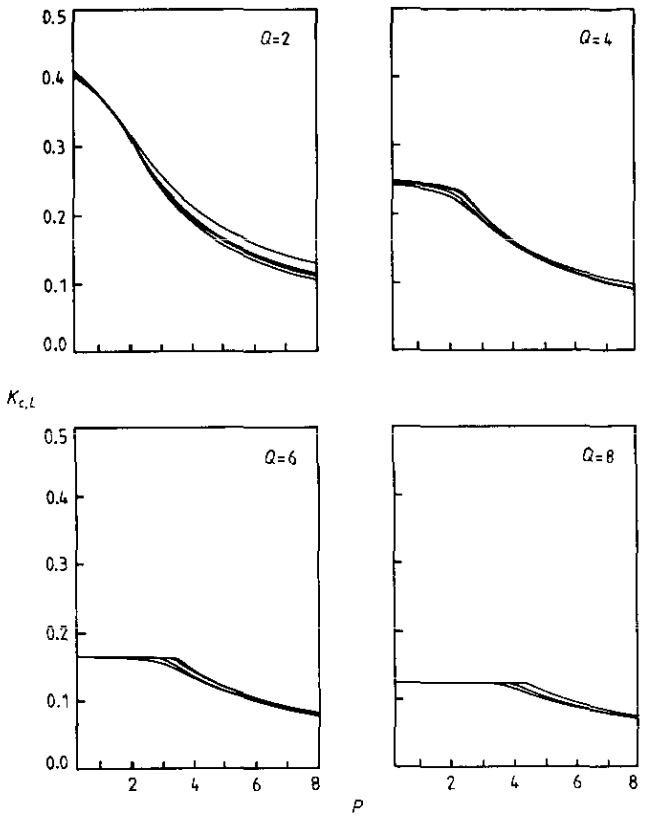

Figure 8. Finite-size estimates of the critical line, $K_{c,L}(P)$, for strips of width L = 4, 5, 6 and 7 at different values of Q.

(figure 10 in particular) are not precise enough to confirm this shift.

Another interesting question is whether or not there is a shift in the adsorption temperature, T_A, due to monomer–monomer interactions in the bulk. From figures 6–10, there is clear evidence that the critical value $Q_c^{Sp} = \exp(\varepsilon_S/k_B T_A)$ increases as P increases, as shown schematically in figure 5. Hence, the adsorption temperature is lowered by the effects of attractive solvent-induced interactions in the bulk.

5. The ordinary-Θ point

We now investigate the extent to which strip calculations can elucidate the fixed-point structure in the parameter space of the model exhibiting both adsorption and collapse transitions. The new fixed-points of interest are (i) the ordinary-Θ fixed-point, which governs the behaviour on the Θ line for $Q < Q_c^{\Theta,Sp}$, and (ii) the special-Θ fixed-point, which describes the adsorption transition of a Θ polymer. Both have analogues in the tricritical O(n) model in the limit $n \to 0$ [30,33].

Duplantier and Saleur have calculated exponents for a SAW with nearest-neighbour interactions and a special subset of next-nearest-neighbour interactions in two dimensions using Coulomb gas methods [34]. They found the bulk tricritical exponents

$$\nu^{\Theta'} = 4/7 \qquad \phi^{\Theta'} = 3/7 \qquad \gamma^{\Theta'} = 8/7 \tag{40}$$

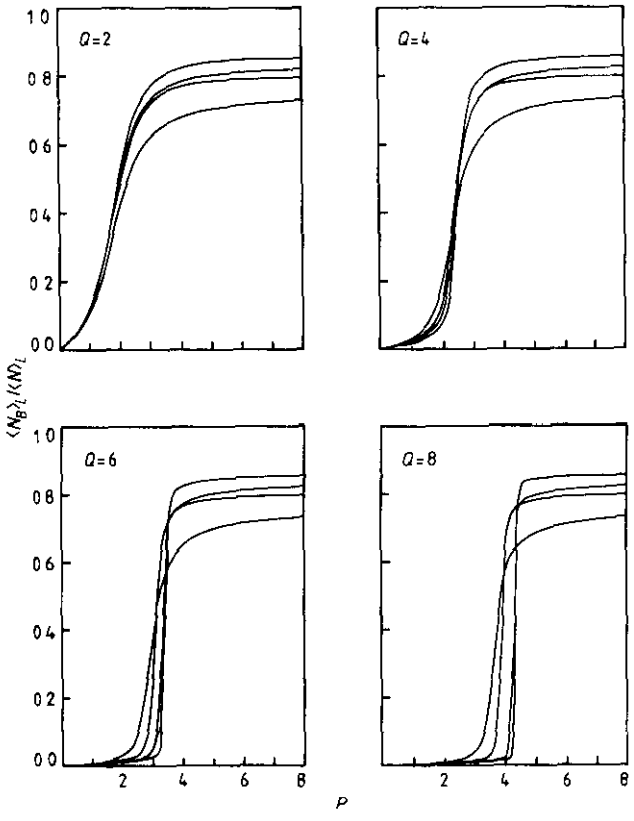

Figure 9. The fraction of bonds at the critical fugacity, $\langle N_B\rangle_L / \langle N\rangle_L$, for strips of width $L = 4, 5, 6$ and 7 at different values of Q. For small values of Q, the variation with P is continuous, while for larger Q the curves suggest a discontinuous change at the unbinding transition in the thermodynamic limit.

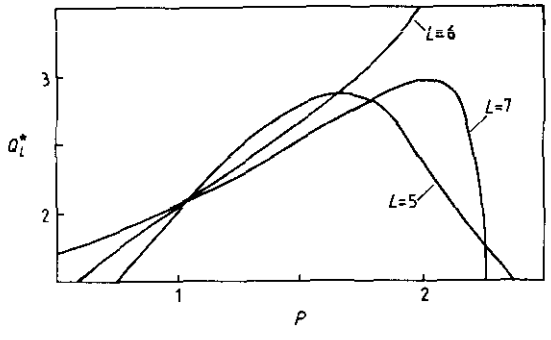

Figure 10. Estimates of the line $Q_L^*(P)$ obtained from equations (38) and (39). For $P \gtrsim 1.6$, the data show severe parity and finite-size effects, but the results for strips of odd parity appear to cross over from the adsorption to the Θ line in the parameter space.

and the ordinary surface exponents

$$\eta_{\parallel}^{\Theta',\mathrm{Ord}} = 0 \qquad y_S^{\Theta',\mathrm{Ord}} = 2/3. \tag{41}$$

The notation Θ' distinguishes this point from the Θ point where conventionally only

nearest-neighbour interactions are included. The question of whether the Θ and Θ' points are in the same universality class has been a subject of debate [35–38] and has stimulated new numerical work [14,39–41]. Numerical evidence appears to show that the bulk exponents at the two points are the same. However, a study of the ordinary surface exponents at the Θ point by Seno and Stella [14,38] revealed differences with the predictions of Duplantier and Saleur.

Seno and Stella performed Monte Carlo enumerations of the number of SAW attached to a *free* surface. At the Θ point they found $\gamma_1^{\Theta,\mathrm{Ord}} = 0.57 \pm 0.08$ and $\gamma_{11}^{\Theta,\mathrm{Ord}} = -0.53 \pm 0.10$, compared with the values $\gamma_1^{\Theta',\mathrm{Ord}} = 8/7$ and $\gamma_{11}^{\Theta',\mathrm{Ord}} = 4/7$ for the Θ' point. From 'plausible assumptions' about the underlying conformal field theory (criticized in [38,40]), they then *conjectured* the exact result

$$\eta_{\parallel}^{\Theta,\mathrm{Ord}} = 2 \qquad \text{in two dimensions.} \tag{42}$$

We also note that Burkhardt and Cardy [42] have given heuristic arguments to show that $x_{\mathrm{S}}^2 = d$ at an ordinary transition. Under rather general assumptions they also derived the result $x_{\mathrm{S}}^2 = 2$ in two dimensions using conformal invariance. This suggests that

$$y_{\mathrm{S}}^{\Theta,\mathrm{Ord}} = -1 \qquad \text{in two dimensions} \tag{43}$$

which is at variance with the value at the Θ' point, (41).

To locate the ordinary-Θ fixed-point, we followed the loci of the ordinary and Θ fixed-points in the parameter space, assuming that the curves would cross at the ordinary-Θ fixed-point. Of course, this method is far from satisfactory, but we were not able to generate transfer matrices for enough strip widths to uniquely define the fixed-point, for example, from the solution of a set of three-parameter renormalization equations.

Estimates of the coordinates of the ordinary line, $K_L^\star(P)$ and $Q_L^\star(P)$, follow from the solutions of the three-strip renormalization equations (equations (26) of section 3) but with strip widths of the same parity (i.e. $L, L-2, L-4$). $Q_L^\star(P)$ is shown in figure 11(a). Estimates of the coordinates of the Θ line, $K_L^\star(Q)$ and $P_L^\star(Q)$, were obtained from the solutions of the two-length, two-strip renormalization equations (compare (38) and (39))

$$L^{-1}\xi_L^{\parallel,1}\left[K_L^\star(Q), P_L^\star(Q)\right] = (L-2)^{-1}\,\xi_{L-2}^{\parallel,1}\left[K_L^\star(Q), P_L^\star(Q)\right] \tag{44}$$

$$L^{-1}\xi_L^{\parallel,2}\left[K_L^\star(Q), P_L^\star(Q)\right] = (L-2)^{-1}\,\xi_{L-2}^{\parallel,2}\left[K_L^\star(Q), P_L^\star(Q)\right]. \tag{45}$$

$P_L^\star(Q)$ has been superimposed onto the graph in figure 11(a). From the graph, we estimate the coordinates of the crossing point as

$$\left(P_{\mathrm{c}}^{\Theta,\mathrm{Ord}}, Q_{\mathrm{c}}^{\Theta,\mathrm{Ord}}\right) = (1.95 \pm 0.05, 0.3 \pm 0.1). \tag{46}$$

The value of $P_{\mathrm{c}}^{\Theta,\mathrm{Ord}}$ is in good agreement with the Monte Carlo estimate of Meirovitch and Lim [41], $P_{\mathrm{c}} = 1.93 \pm 0.01$, for the *bulk* Θ point.

In principle, estimates of the surface scaling dimensions at the ordinary-Θ fixed-point now follow from the amplitudes of the correlation lengths. Figure 11(b) shows the correlation length amplitude along the ordinary line

$$A_L^1(P) = \frac{2L}{\pi\xi_L^{\parallel,1}\left[K_L^\star(P), Q_L^\star(P)\right]}. \tag{47}$$

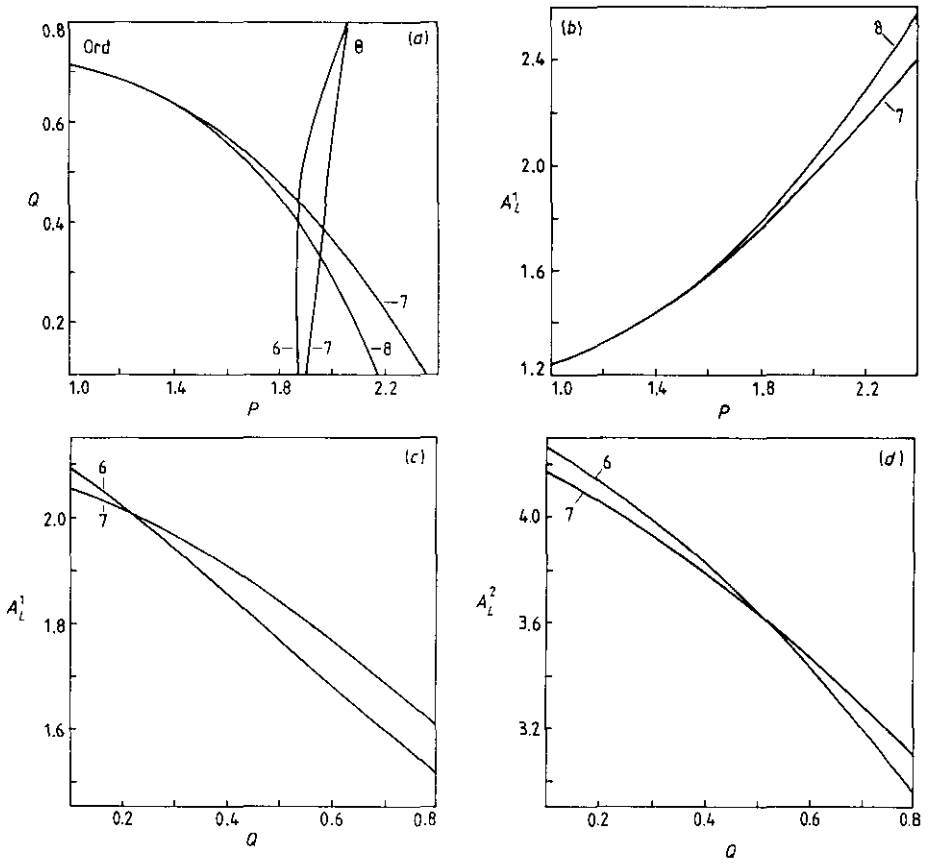

Figure 11. (a) Finite-size estimates of the lines of fixed-points in the critical surface, $K = K^*(P, Q)$, projected onto the (P, Q) plane. The lines of ordinary fixed-points, $Q_L^*(P)$, and the lines of Θ fixed-points, $P_L^*(Q)$, are labelled Ord and Θ, respectively. Each line is marked by the largest strip width used in the phenomenological renormalization calculation of its coordinates. (*b*) The correlation length amplitude along the ordinary line, $A_L^1(P)$. (*c*) The correlation length amplitudes on the tricritical Θ line, $A_L^i(Q)$, for $i = 1$ and (*d*) the same for $i = 2$.

Although the curves do not cross, from the value of $P_c^{\Theta,\mathrm{Ord}}$ we estimate $A_L^1(P_c^{\Theta,\mathrm{Ord}}) = 2.0 \pm 0.1$. Figures 11(*c*) and (*d*) show the amplitudes along the Θ line

$$A_L^i(Q) = \frac{2L}{\pi \xi_L^{\parallel,i}[K_L^*(Q), P_L^*(Q)]} \tag{48}$$

for $i = 1$ and 2. The curves in figure 11(*c*) cross at $Q \sim 0.2$ and the values of $A_L^1(Q)$ at the crossing-point and at $Q_c^{\Theta,\mathrm{Ord}}$ are consistent with the estimate $A_L^1(Q_c^{\Theta,\mathrm{Ord}}) = 2.0 \pm 0.1$. The curves in figure 11(*d*) also cross, at $Q \sim 0.5$, and the values of $A_L^2(Q)$ at the crossing-point and at $Q_c^{\Theta,\mathrm{Ord}}$ suggest that $A_L^2(Q_c^{\Theta,\mathrm{Ord}}) = 3.8 \pm 0.2$.

Our results therefore suggest the values

$$\eta_{\parallel}^{\Theta,\mathrm{Ord}} = 2.0 \pm 0.1 \qquad x_S^2 = 1.9 \pm 0.1 \tag{49}$$

at the ordinary-Θ fixed-point, which supports the conjecture of Seno and Stella (42) and agrees with the general result $x_S^2 = 2$ at an ordinary transition. However, the

apparent strong agreement with expected values may be fortuitous and we hope to stimulate further work, perhaps using conformal invariance techniques.

A similar attempt to locate the special-Θ fixed-point, by following the loci of the special and Θ fixed-points in the parameter space, was not successful. Distortions in the crossover trajectories were very pronounced, as is evident from figure 10, and it proved impossible to interpret the finite-size data [43].

6. Discussion and conclusions

In summary, we have used the transfer matrix technique to study a lattice model of polymer adsorption and collapse. We have considered the standard model of a self-avoiding walk with adsorbing boundaries and introduced attractive nearest-neighbour interactions. The numerical results show the existence of a multicritical point where the adsorption and collapse transitions coincide. There is also clear evidence that the collapse transition lowers the adsorption temperature and that the order of the adsorption transition changes from second to first order as the monomer–monomer interactions increase in strength. The resulting phase diagram, shown schematically in figure 5, agrees qualitatively with that of Bouchaud and Vannimenus [9] who performed real-space renormalization calculations for a polymer model incorporating surface adsorption and attractive interactions on the three-dimensional Sierpinski gasket.

The universality class of a polymer chain at the Θ point in two dimensions has been much debated following the determination of the *exact* tricritical exponents at the Θ' point by Duplantier and Saleur [34]. The point at issue is whether or not the appealing geometrical model studied by Duplantier and Saleur, which has both nearest-neighbour and a special subset of next-nearest-neighbour interactions, is in the same universality class as the standard model with only nearest-neighbour interactions. To investigate this point, we have studied the amplitudes of the correlation lengths for one and two polymers at the ordinary-Θ fixed-point. The resulting estimates of the surface scaling dimensions support the recent conjecture of Seno and Stella [14, 38] that the *surface* critical behaviour at the Θ and Θ' points is different and that $\eta_{\parallel}^{\Theta,\mathrm{Ord}} = 2$.

The surface critical behaviour at the collapse–adsorption multicritical point is very interesting. Unfortunately, phenomenological renormalization calculations proved extremely difficult to perform because of strong parity and finite-size effects and we were unable to give reliable estimates of the critical exponents at the special-Θ fixed-point. Diehl and Eisenriegler [30] have calculated expressions for the surface critical exponents at the special fixed-point of the tricritical O(n) model using sophisticated field-theoretic techniques; putting $n = 0$ into the $\epsilon = 3 - d$ expansions gives the exponents for a Θ polymer at the collapse–adsorption multicritical point. However, the expansions converge poorly and are not expected *a priori* to give reliable estimates when $\epsilon = 1$. We hope that further progress may be made using conformal invariance and related techniques.

In view of the inherent difficulties with transfer matrix calculations for the self-avoiding walk model at the Θ point, we went on to study a much simpler *directed* model which also exhibits *both* adsorption and collapse transitions [10]. Directed models of polymer adsorption have been studied in detail by Privman and co-workers [44, 45] and may be of some physical interest when polymer adsorption takes place in the presence of shear flow parallel to the surface. In fact, the directed model of polymer

adsorption may be solved analytically [45] and the finite-size scaling properties of the model in the strip geometry can be calculated [10,46].

If attractive nearest-neighbour interactions are introduced, a full analytic treatment of the model is no longer possible. However, a numerical transfer-matrix study [10] proved a great deal easier than in the case of the isotropic self-avoiding walk because of the possibility of probing large strip widths ($L \lesssim 50$) and the regular convergence of the results with increasing L. The results revealed the same generic features as the model we have studied in this article: (i) there is a multicritical point where the adsorption and collapse transitions coincide, and (ii) the adsorption transition is second order above the collapse–Θ temperature and first order below.

We found that the position of the adsorption transition could be estimated from the point where the finite-size critical fugacity curves cross. Furthermore, the numerical study obtained results for the position of the multicritical point of the directed model that were independent of L. The *exact* values of the thermodynamic parameters at this multicritical point have subsequently been calculated [47].

Although the simple directed model shows the same general behaviour as the isotropic self-avoiding walk model, we have proved analytically that there is no enhancement of the Θ temperature in the presence of an adsorbing surface [10,47]. This may be due to the anisotropic nature of the collapse transition of the directed polymers. However, one of the most interesting questions of physical interest remains whether or not a shift in Θ is present in more realistic models. A parallel study of a related geometrical model of polymer collapse [13] did show a *surface-induced* stabilization of the collapsed phase near the multicritical point in the phase diagram. Unfortunately, the results of section 4 are not sufficiently accurate to resolve this point for the self-avoiding walk model.

We hope that these results will stimulate further theoretical work on problems involving strongly interacting polymers at interfaces. The recent simulation studies of Seno and Stella [14] and Meirovitch and Lim [41] of the two-dimensional self-avoiding walk model at the Θ point, both in the bulk and at a *free* surface, have given very precise results. Large-scale Monte Carlo simulations of the model at an adsorbing surface, developing the earlier work of Eisenriegler, Binder and Kremer [19] for polymers above the Θ point, might be able to answer detailed questions about the enhancement of the Θ temperature and the critical exponent values at the collapse–adsorption multicritical point in both two and three dimensions. Van Dieren and Kremer's study [48] of a simplified three-dimensional model of adsorption at the Θ point offers a promising start in this direction.

Acknowledgments

ARV acknowledges financial support from SERC and AFRC through the award of a CASE studentship and the Theory and Computational Science Group at FRIN for their hospitality during visits in 1988–9 when much of this work was carried out. We would also like to thank Koos Rommelse for independently checking some transfer matrix results and Aleks Owczarek for clarifying discussions and comments on the manuscript.

References

[1] Napper D 1983 *Polymeric Stabilization of Colloidal Dispersions* (New York: Academic)

[2] Bee R D, Richmond P and Mingins J (eds) 1989 *Food Colloids* (London: Royal Society of Chemistry)
[3] Houslay M D and Stanley K K 1982 *Dynamics of Biological Membranes* (New York: Wiley)
[4] Williams C, Brochard F and Frisch H L 1981 *Ann. Rev. Phys. Chem.* **32** 433
[5] Binder K and Kremer K 1985 *Scaling Phenomena in Disordered Systems* ed R Rynn and A Skjeltorp (New York: Plenum) p 525
[6] de Gennes P G 1987 *Adv. Colloid Interface Sci.* **27** 189
[7] Cardy J L 1987 *Phase Transitions and Critical Phenomena* vol 11, ed C Domb and J L Lebowitz (New York: Academic) p 55
[8] Duplantier B *1988 5th IFF-ILL Workshop: Molecular Basis of Polymer Networks October 1988, Julich* (Berlin: Springer)
[9] Bouchaud E and Vannimenus J 1989 *J. Physique* **50** 2931
[10] Veal A R, Yeomans J M and Jug G 1990 *J. Phys. A: Math. Gen.* **23** L109
[11] Saleur H 1986 *J. Stat. Phys.* **45** 419
[12] Guim I and Burkhardt T W 1989 *J. Phys. A: Math. Gen.* **22** 1131
[13] Cattarinussi S and Jug G 1990 *J. Phys. A: Math. Gen.* **23** 2701
[14] Seno F and Stella A L 1988 *J. Physique* **49** 739; 1988 *Europhys. Lett.* **7** 605
[15] Klein D J 1980 *J. Stat. Phys.* **23** 561
Enting I G 1980 *J. Phys. A: Math. Gen.* **13** 3713
Derrida B 1981 *J. Phys. A: Math. Gen.* **14** L5
[16] de Gennes P G 1979 *Scaling Concepts in Polymer Physics* (Icatha, NY: Cornell University Press)
[17] Cardy J L 1984 *J. Phys. A: Math. Gen.* **17** L385; 1984 *Nucl. Phys.* B **240** 514
[18] Duplantier B and Saleur H 1986 *Phys. Rev. Lett.* **57** 3179
[19] Eisenriegler E, Kremer K and Binder K 1982 *J. Chem. Phys.* **77** 6296
[20] Binder K 1983 *Phase Transitions and Critical Phenomena* vol 8, ed C Domb and J L Lebowitz (New York: Academic) p 1
[21] Barber M N 1983 *Phase Transitions and Critical Phenomena* vol 8, ed C Domb and J L Lebowitz (New York: Academic) p 145
[22] Burkhardt T W, Eisenriegler E and Guim I 1989 *Nucl. Phys.* B **316** 559
[23] Guttmann A J and Enting I G 1988 *J. Phys. A: Math. Gen.* **21** L165
[24] Burkhardt T W and van Leeuwen J M J 1982 *Real-Space Renormalisation (Topics in Current Physics 30)* ed T W Burkhardt and J M J van Leeuwen (Berlin: Springer) p 1
[25] Derrida B and Herrmann H J 1983 *J. Physique* **44** 1365
[26] Privman V and Fisher M E 1983 *J. Phys. A: Math. Gen.* **16** L295
[27] Derrida B and Stauffer D 1985 *J. Physique* **46** 1623
[28] de Gennes P G 1975 *J. Phys. Lett. France* **36** L55; 1978 *J. Physique Lett.* **39** L299
[29] Duplantier B 1986 *Europhys. Lett.* **1** 491; 1987 *J. Chem. Phys.* **86** 4233
[30] Diehl H W and Eisenriegler E 1987 *Europhys. Lett.* **4** 709
Eisenriegler E and Diehl H W 1988 *Phys. Rev.* B **37** 5257
[31] Duplantier B and Saleur H 1987 *Nucl. Phys.* B **290** 291
[32] Dill K A and Alonso D O V 1988 *Protein Structure and Protein Engineering (Colloq. Mosbach 1988)* (Berlin: Springer) p 51
[33] Speth W 1983 *Z. Phys.* B **51** 361
[34] Duplantier B and Saleur H 1987 *Phys. Rev. Lett.* **59** 539
[35] Coniglio A, Jan N, Majid I and Stanley H E 1987 *Phys. Rev.* B **35** 3617
[36] Saleur H and Duplantier B 1987 *Phys. Rev. Lett.* **58** 2325
[37] Poole P H, Coniglio A, Jan N and Stanley H E 1988 *Phys. Rev. Lett.* **60** 1203
Duplantier B and Saleur H 1988 *Phys. Rev. Lett.* **60** 1204
[38] Seno F, Stella A L and Vanderzande C 1988 *Phys. Rev. Lett.* **61** 1520
Duplantier B and Saleur H 1988 *Phys. Rev. Lett.* **61** 1521
[39] Poole P H, Coniglio A, Jan N and Stanley H E 1989 *Phys. Rev.* B **39** 495
[40] Duplantier B and Saleur H 1989 *Phys. Rev. Lett.* **62** 1368
[41] Meirovitch H and Lim H A 1989 *Phys. Rev. Lett.* **62** 2640
Duplantier B and Saleur H 1989 *Phys. Rev. Lett.* **62** (1989) 2641
Meirovitch H and Lim H A 1989 *J. Chem. Phys.* **91** 2544
[42] Burkhardt T W and Cardy J L 1987 *J. Phys. A: Math. Gen.* **20** L233
[43] Veal A R 1990 *DPhil. thesis* Oxford University

[44] Privman V and Švrakić N M 1989 *Directed Models of Polymers, Interfaces, and Clusters: Scaling and Finite-Size Properties (Lecture Notes in Physics* **338***)* (Berlin: Springer)
[45] Privman V, Forgacs G and Frisch H L 1988 *Phys. Rev.* B **37** 9897
Forgacs G, Privman V and Frisch H L 1989 *J. Chem. Phys.* **90** 3339
[46] Privman V and Švrakić N M 1988 *Phys. Rev.* B **37** 3713
[47] Binder P-M, Owczarek A L, Veal A R and Yeomans J M 1990 *J. Phys. A: Math. Gen.* **23** L975
Foster D P 1990 *J. Phys. A: Math. Gen.* **23** L1135
[48] van Dieren F and Kremer K 1987 *Europhys. Lett.* **4** 569